

# Quantitative Magnetic Resonance Imaging With The Mixed Turbo Spin-echo Pulse Sequence: A Validation Study

M Jensen, S Caruthers, H Jara

## Citation

M Jensen, S Caruthers, H Jara. *Quantitative Magnetic Resonance Imaging With The Mixed Turbo Spin-echo Pulse Sequence: A Validation Study*. The Internet Journal of Radiology. 2000 Volume 2 Number 1.

## Abstract

The quantitative accuracy of images generated with mixed turbo spin echo (mix-TSE) pulse sequence and model-conforming quantitative algorithms is tested experimentally with a multi-sample phantom. Quantitative T1 and T2 accuracy within a few percent is demonstrated for samples representing tissues with MR relaxation times spanning the full T1 and T2 biologic ranges, with the exception of T2 measurements of simple fluids with very long T2 relaxation times. To correct this problem, a simple approach based on the known proportionality  $T1 \propto T2$  exhibited by simple fluids is proposed. The results show that the mix-TSE pulse sequence can be used to generate accurate and high quality quantitative image sets with large anatomic coverage and near isotropic high spatial resolution. In conclusion, the mix-TSE pulse sequence could become a valuable tool for clinical applications of quantitative MR imaging.

## INTRODUCTION

### QUANTITATIVE MRI PRINCIPLES

Most MR images generated with current techniques are qualitative in that pixel values contain a mixture of information stemming from both image tissues and experimental conditions used during the scan (examples of this are receiver gain and coil sensitivity). The defining aspect of quantitative image information, as opposed to qualitative image information, is that quantitative pixel values do not contain superfluous experimental information and are therefore primarily tissue specific. Since the advent of MRI, quantitative MR images, often called maps, representing a large number of tissue properties have been generated, principally including images of proton density (PD) (Ref. 1,2), longitudinal magnetization recovery time (T1) (Ref. 1), spin-echo transverse magnetization recovery time (T2) (Ref. 2), flow velocity (Ref. 4), and self-diffusion coefficient (D) (Ref. 5).

All known techniques for quantitative MR imaging (Q-MRI) consist of the application of at least two MRI scans applied under identical conditions except for the value of one scan parameter that affects the MRI signal in a known form. The relaxation of tissue is modeled with the laws of MRI physics to relate this pulse sequence parameter to the tissue property that the Q-MRI technique seeks to determine. For example, to determine T2, two scans that are identical except for their

echo time (TE) values are used. On a pixel-by-pixel basis, Q-MRI information is then computed using an algorithm based on the physics model of the relaxation differences between the measurements performed in the two acquisitions. Using such algorithms, estimates of the specific tissue properties (e.g. PD, T1, T2, etc.) at every pixel are generated, thus leading to the generation of Q-MR images. In summary, a quantitative MRI technique is a multi-phase process that firstly consists in the acquisition of at least two sets of source images directly acquired with a Q-MRI pulse sequence. In the second phase, which is computational, these source images are used as input to a post-processing computer algorithm to generate the Q-MR images. Throughout this paper we will refer to the acquisition pulse sequence and the quantitative algorithms as the Q-MRI pulse sequence and the Q-MRI algorithms, respectively.

### CURRENT LIMITATIONS OF Q-MRI

The use of Q-MRI techniques is not widely spread in clinical practice for reasons relating to the practicality of the scanning technique and to the poor image quality many times achieved with these. From a practical perspective, many of the Q-MRI pulse sequences previously used by other researchers are scan time inefficient resulting in lengthy exams. Furthermore, many of the Q-MRI algorithms that have been used by other researchers can generate images with poor signal to noise and/or high incidence of

pixel dropout artifacts (i.e. bright spots in random positions) throughout the images.

## PURPOSE OF WORK

A pulse sequence known as the mixed turbo spin-echo (mix-TSE), which is practical from a clinical operations standpoint is studied in this work. First, because the mix-TSE pulse sequence employs TSE readouts (Ref. 6), the pulse sequence is inherently fast. Second, using the mix-TSE pulse sequence is simple operationally. The mixed scanning principle (Ref. 7) combines two multi-echo, inversion recovery acquisitions with different inversion times, thus generating several images per slice with different levels of T1 and T2 weightings. Hence, when properly optimized, the application of a single mixed turbo spin-echo scan can be used to generate enough imaging data to compute Q-MR images representing PD, T1, and T2 with large anatomic coverage and high spatial resolution, yet in a clinically reasonable scan time. Furthermore, when this source imaging data is post-processed with a newly developed type of Q-MRI algorithm known as the model-conforming algorithm (Ref. 8), Q-MR images practically devoid of pixel dropout artifacts can be generated. The rationale of model-conforming Q-MRI algorithms is to automatically detect, based on the noise level in the image, the pixels where the physical model is not applicable, such as cortical bone, air, and other non-MR active materials. These pixels representing tissues/materials that are not accurately described by the physics model are set to a predetermined value. In parallel, for pixels that are MR active, Q-MRI values are calculated with the appropriate inversion formula of the physics model. Although this specific Q-MRI technique, mix-TSE pulse sequence analyzed with the model-conforming algorithm, is very promising for the reasons stated above, its quantitative accuracy has not been proven. It is therefore the purpose of this work to examine the quantitative accuracy of mix-TSE/model-conforming algorithm data within the known biological ranges for T1 and T2 using a previously validated technique (mix-CSE / RLSQ) as a reference.

## METHODS AND MATERIALS

### EQUIPMENT

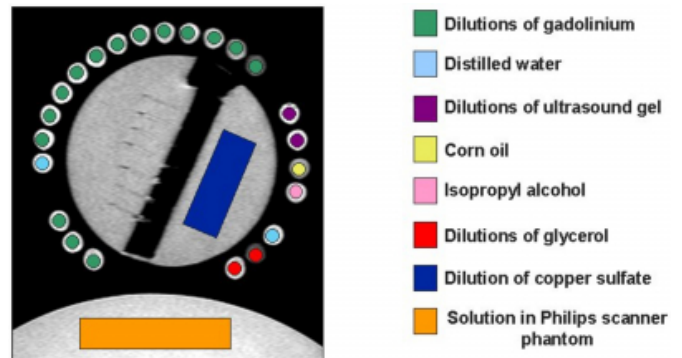
All images were acquired with a 1.5 T superconducting MR imaging system (Gyrosan ACS-NT Philips Medical Systems of North America) with a maximum gradient of 23 mT m<sup>-1</sup> and a maximum slew rate of 105 mT m<sup>-1</sup> ms<sup>-1</sup>. Phantom experiments and human studies in the head were

performed with standard equipment, the body coil and the head coil, respectively.

A multi-sample phantom was constructed containing solutions with T1 and T2 relaxations varying over the biologic range (figure 1). The list of chemicals in the phantom solutions includes dilutions of gadopentetate dimeglumine (Magnevist), ultrasound transmission gel (E-Z Gel), isopropyl alcohol, glycerol (EM Science), copper sulfate, sodium chloride, and corn oil.

### Figure 1

Figure 1: Cross sectional image of calibration phantom composed of several fluid-filled containers. An overlying color-coding shape has been applied to further categorize the solution type and region of measurement. This phantom contains materials spanning the T1 and T2 relaxation times of the biologic range.



Model-conforming algorithms were programmed in MathCAD 2000/2001 (Mathsoft, Cambridge, MA) operating on a windows-based personal computer. Pearson's correlation coefficient (r<sup>2</sup>) was calculated in MathCAD to compare Q-MRI measurements.

## PULSE SEQUENCES AND COMPUTER ALGORITHMS FOR PD, T1, AND T2 Q-MRI

The mixed conventional spin-echo (mix-CSE) pulse sequence was originally described by in den Kleef and Cuppen (Ref. 7) at a time early in the development of MR imaging when the faster hybrid data acquisition methods used today (FSE and TSE) were not widely available. Hybrid scanning methods are faster because several lines of Fourier space data are acquired per pulse sequence cycle (TR). In this terminology, conventional scanning methods represent the limiting case of hybrid methods in which only one line is acquired per cycle.

The mix-CSE pulse sequence is a combination of two multi-echo pulse sequences that are applied in tandem after a 180-

degree inversion pulse (see figure 2A), resulting in a single MRI scan (with the same receiver gain) with which images of several T1 and T2 contrast weightings and identical pixel positioning are generated. When the mixed scanning principle is combined with a conventional data acquisition scanning method, scans result that are not clinically practical from the perspectives of scan time and anatomic coverage. Such limitations can be overcome by implementing the mixed principle together with the fast or turbo spin-echo principle as illustrated in figure 2B, which greatly increase the scan time efficiency. For example, the mix-TSE pulse sequence of interest in this work can be used to generate PD, T1, and T2 Q-MRI data sets of a human head, with full and gapless anatomic coverage (80 slices, 2.5 mm thickness, NSA = 1), in approximately 10 minutes with a standard clinical MRI scanner. The pulse sequence parameters used in this validation study with phantoms are slightly different (see table 1) but do illustrate the increased scan time efficiency of the mix-TSE pulse sequence.

**Figure 2**

Figure 2: Mix-CSE and mix-TSE pulse sequence timing diagrams. The two pulse sequences share a common architecture. The improved scan time efficiency of the mix-TSE pulse sequence stems from the use of turbo spin echo readouts with which several lines in k-space are acquired within a single pulse sequence cycle.

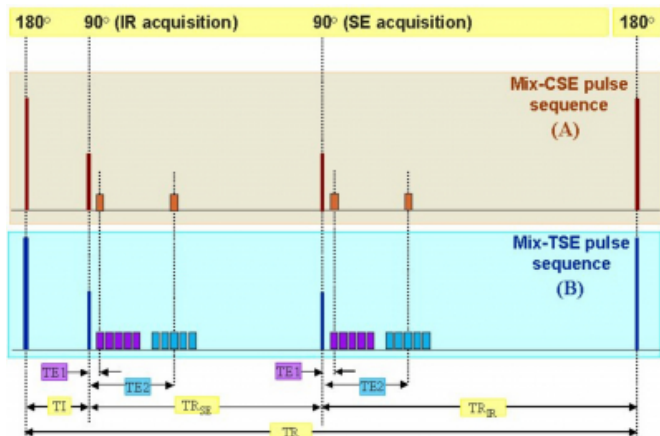


**Figure 3**

Table 1: Pulse sequence parameters used in validation study with phantoms. Note that NSA = 2 was used thus lengthening the overall scan times by a factor of two. Use of NSA = 2 is not necessary in clinical applications of the mix-TSE such as the head scan described in the text above.

Scanner Parameter	mix-CSE	mix-TSE
No. of 2D slices	1	80
Slice thickness	4 mm	2.5 mm
No. signals acquired (NSA)	2	2
Acquisition matrix (FE dir.)	128 pixels	256 pixels
Field of view (FOV)	240 mm	240 mm
Scan percent	50%	50%
Echo times (TE <sub>1,2</sub> and TE <sub>1,2sp</sub> )	7.1 / 113	8.1 / 113
Echo train length (ETL)	1 k-line per echo	9 k-lines per echo
Repetition time (TR <sub>sp</sub> /TR <sub>0</sub> )	4300 / 5000 ms	8688 / 9300 ms
Scan time	17:03 min	15:39 min

The original work by In den Kleef and Cuppen (Ref. 7) also involved the use of a type of Q-MRI algorithms, which these researchers named RLSQ algorithms, combining pixel value ratio and linear squared fitting operations. These algorithms, which are standard in the software of the MRI equipment used (Gyrosan ACS-NT, Philips Medical Systems of North America) and whose accuracy has been validated by others (Ref. 8), were also used to compute T1 and T2 Q-MR images. In summary, a total of six Q-MR images per slice were studied as listed in table 2.

**Figure 4**

Table 2: Data set classification of the six Q-MR images analyzed (T1 and T2 for each set).

Data set name	Pulse sequence	Q-MRI algorithm	Tissue properties	Comment
RLSQ CSE T1,T2	Mix-CSE	RLSQ	T1, T2	Used as reference
RLSQ TSE T1,T2	Mix-TSE	RLSQ	T1, T2	Scanner generated
MC TSE T1,T2	Mix-TSE	Model-conforming	T1, T2	Developed for this work

**DATA ANALYSIS METHODOLOGY**

According to MR theory, T1 is a much better defined quantity than T2 because the T2 decay of the signal can be influenced not only by the refocusing RF pulses, but also from signal interference effects, which increase for increasing voxel size. In other words, T1 is approximately independent of voxel size and of pulse sequence type used (gradient spin-echo vs. turbo spin-echo). Furthermore, since the mix-CSE RLSQ has been previously validated quantitatively, in this work the RLSQ CSE T1 data is used as the parametric independent variable (i.e. ordinate in all graphs).

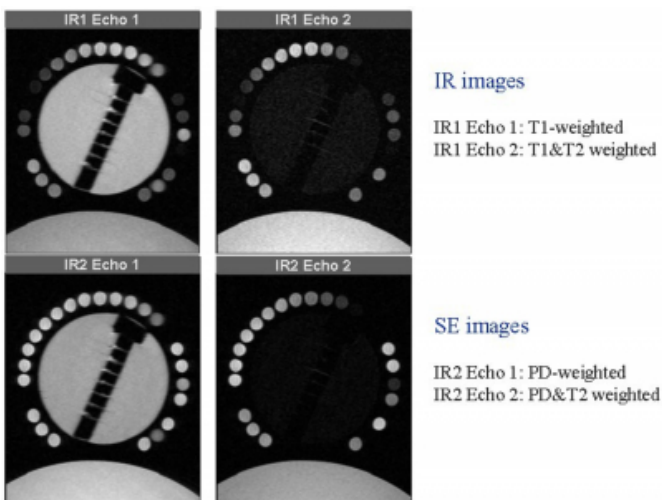
Furthermore, analysis for the T2 calculations is also performed using RLSQ CSE T1 as the independent variable. In this way, measurements grouped in different compartments of the T1, T2 plane can be analyzed

separately. The T1, T2 plane is naturally divided between physical and unphysical domains by a diagonal line ( $T2 = T1$ ). The unphysical domain ( $T2 > T1$ ) refers to the region above the line, which would represent substances in which T2 relaxation occurs at a slower rate than T1 relaxation, thus contradicting NMR theory. According to NMR theory, T1 relaxation and T2 relaxation are both exponential phenomena that occur at different rates, T1 being the slower of the two phenomena. T2 relaxation includes all processes that contribute to T1 relaxation in addition to other signal relaxation phenomena, examples of which are dephasing caused by magnetic field inhomogeneities and also diffusional effects of substances containing magnetic field inhomogeneities. For this theoretical reason, there can be no substances where T2 relaxation is slower than T1 relaxation. Any measurement that contradicts this will therefore be referred to as an unphysical measurement.

The T1 and T2 relaxation data displayed in this work is obtained from region of interest (ROI) measurements that were selected to be as large as possible within each sample area, typically 64 pixels for the small samples and 2200 pixels for the larger samples (see figure 1).

**RESULTS**  
**SOURCE IMAGES**

**Figure 5**  
Figure 3: Phantom source images acquired using the mix-TSE pulse sequence. Note the different levels of T1 weightings between first and second row. Also note that the level of T2 weighting increases from left to right column.



Source images corresponding to one coronal slice in the phantom are shown in figure 3. These images represent four

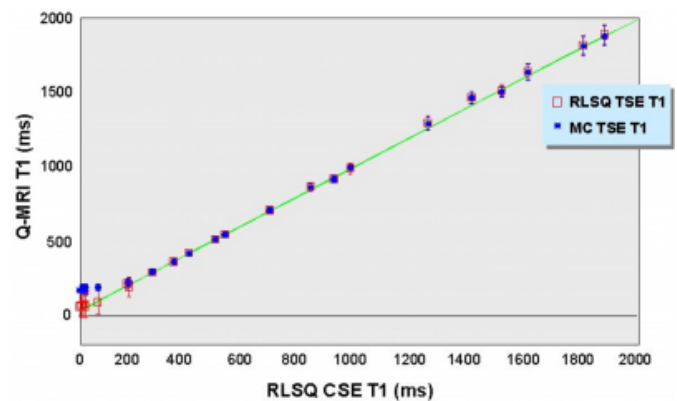
acquisitions performed with same mix-TSE scan, which differ in either the inversion recovery time or the echo time, or both. Otherwise, all other acquisition parameters were identical. In addition, these images have different levels of T1 and T2 weightings and therefore are suitable inputs for the T1 and T2 Q-MRI algorithms of interest to this work.

**QUANTITATIVE ACCURACY**

T1 measurements

ROI measurements of T1 for the several substances of the quantitative phantom are graphed in figure 4 as a function of the independent variable RLSQ CSE T1. The line of identity represents perfect agreement between any measurements in relation to the gold standard used (RLSQ CSE T1). Clearly, the three techniques agree within the experimental error for substances with T1 values above 200 ms. The agreement between the MC TSE T1 and the reference RLSQ CSE T1 is excellent within the biological range ( $r^2 \approx 1$ ) and shows slightly larger deviations over the full range studied ( $r^2 = 0.997$ ). For very short T1 values, at the low end of the biological range (i.e.  $< 200$  ms), a small deviation for the mix-TSE/ model conforming algorithm is observed. This deviation is not observed for the RLSQ TSE T1 measurements, which exhibit the same high correlation coefficient ( $r^2 \approx 1$ ) with respect to the reference RLSQ CSE T1 despite the inclusion of low T1 measurements. Also note that although the techniques exhibit systematically larger errors for T1 values at the high end of the biological range, the uncertainty of the measurements as expressed by one standard deviation is approximately technique independent.

**Figure 6**  
Figure 4: T1 measurements obtained with the three techniques, graphed as a function of increasing T1. The green line indicates the line of identity.





**T2 measurements**

As before, ROI measurements of T2 for the several substances of the quantitative phantom are graphed in figure 5 as a function of increasing T1 obtained with the reference technique (RLSQ mix-CSE). In the following, this data will be examined by separating measurements that fall into several partitions of the T1, T2 plane. First, the data shows excellent agreement between all three T2 Q-MRI techniques for substances with measured T1 values less than 450 ms and T2 less than approximately 500 ms (see purple lines figure 5). In this range of agreement, the correlation coefficients between the three Q-MRI techniques are high ( $r^2 < 0.972$ ) with an exceptional correlation between the MC TSE T2 and RLSQ TSE T2 ( $r^2 @ 1$ ). Furthermore, in this range all T2 measurements exhibit small uncertainties as indicated by the small errors bars. Secondly, in the region defined by T1 greater than 450 ms and T2 greater than approximately 500 ms there is agreement between the three T2 techniques for a few substances, but for most substances large disagreements are observed between the measurements obtained with the TSE techniques in comparison to the corresponding CSE measurements. The T2 TSE measurements of these substances all fall into the unphysical range, as defined above, and exhibit very large error bars (see figure 5).

**Figure 7**

Figure 5: T2 measurements obtained with the three techniques, graphed as a function of increasing T1. The green line indicates the line of identity. Where possible, solution type is labeled in green.

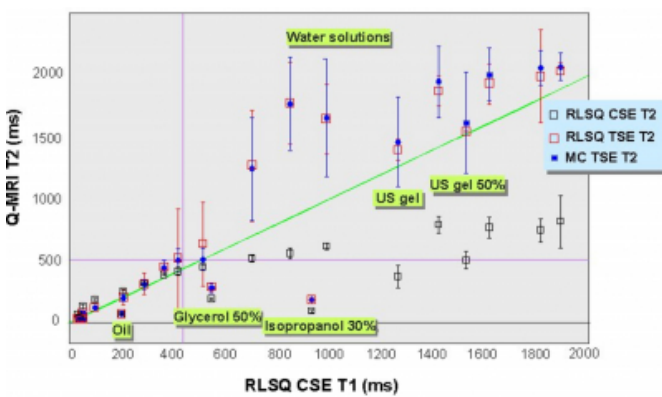


**Image quality**

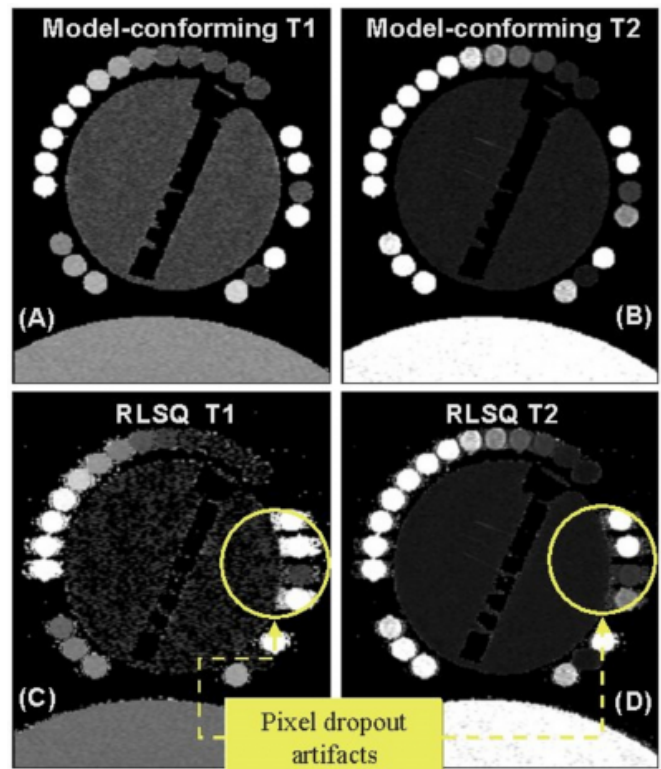
Representative T1 and T2 images obtained with the mix-TSE pulse sequence and the two Q-MRI algorithms (model conforming and RLSQ) are shown in figure 6 below. In agreement with the ROI analysis above, there is excellent

visual agreement between corresponding Q-MR images obtained with the two algorithms as shown by the relative image intensities of the several substances in the phantom.

As shown in figure 6, the dropout artifacts, resulting from the RLSQ algorithm applied to pixels where the NMR model does not apply, can in some instances be severe enough to distort the shape of some features in the image.

**Figure 8**

Figure 6: Representative Q-MR images of the phantom. T1 and T2 Q-MR images derived from a set of coronally acquired TSE source images. T1 (A) and T2 (B) Q-MR images generated with the model-conforming algorithms discussed in this work. Note the low incidence of pixel-dropout artifacts compared to the corresponding Q-MRI images generated with the RLSQ T1 (C) and T2 (D) algorithms.



**DISCUSSION**

Quantitative determination of MR tissue properties (e.g. PD, T1, and T2) on a pixel-by-pixel basis could be important from the stand points of (1) advancing the diagnostic capabilities of MR imaging and (2) standardizing and simplifying clinical MRI operations. Specially promising clinical applications of quantitative MRI are virtual MRI scanning to generate virtual images with any desired contrast weighting and tissue classification in a form analogous to

that of X-ray computed tomography (CT) where the use of the Hounsfield scale is standard practice.

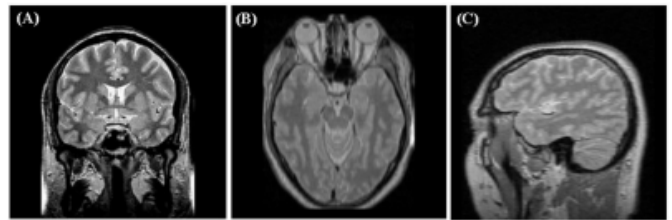
Generation of Q-MR images is a two-step process, namely data acquisition with a pulse sequence and image post processing with a mathematical model that is embodied in the Q-MRI algorithm. The accuracy and the quality of the final product, namely the Q-MR image, can therefore be affected by both imperfections in the pulse sequence and by limitations in the algorithms. The purpose of this work was to test a Q-MRI technique for T1 and T2 accuracy that uses the mix-TSE pulse sequence for the data acquisition and model conforming Q-MRI computer algorithms in the image processing phase. From a clinical standpoint, the mix-TSE pulse sequence is attractive because it is very scan-time efficient, thus permitting scans with large anatomic coverage and high spatial resolution. The near isotropic nature of the source imaging data, as illustrated in figure 7, allows high quality axial and sagittal orthogonal reformations. If Q-MRI becomes standard practice, conceivably the mathematical model could be embedded directly into the Fourier transform image reconstruction algorithm.

The experimental results show that this technique produces accurate T1 measurements within the biologic range. The results also show that T2 measurements are accurate for T2 values of less than about 500 ms, thus covering all known gel-like biologic tissues. On the other hand, the long T2 values of most simple fluids in the human body (e.g. CSF, bile, synovial fluid) could be overestimated with this technique. These inaccuracies and large uncertainties most likely result from using an echo time difference ( $TE_2 - TE_1 = 106$  ms) that is too short for the observation of significant amplitude decay in data that contains noise. In such a short time, the exponential signal decay of a substance with  $T_2=500$  ms is approximately 20% and since the SNR level in the two source images used for quantitative analysis is approximately 10% for each, quantitative inaccuracies secondary to noise in the source images are to be expected. Although scanning with a longer echo time difference could reduce these long-T2 inaccuracies, such an approach is likely to decrease the T2 accuracy for the other non-simple soft tissues exhibiting T2 times of typically less than 100 ms. Another approach for improving the accuracy of T2 measurements of simple fluids is to use the linear relationship that exists between T1 and T2 values of simple fluids. In this form, since the T1 measurements for simple fluids are accurate with this technique, the corresponding T2

values can be easily and accurately determined by a simple multiplication. Such an approach is currently under investigation and the results will be reported separately.

**Figure 9**

Figure 7: One of a set of 80 source images of the human head (A) of a healthy volunteer acquired in the coronal plane. From these, high-quality orthogonal reformations in the axial (B) and sagittal (C) planes can be constructed.



**CONCLUSION**

The mix-TSE pulse sequence can yield scans suitable for Q-MRI post processing and are quantitatively accurate for T1 and T2 at the pixel level throughout their respective biologic ranges. The mix-TSE pulse sequence is also clinically practical from the standpoints of anatomic-coverage-to-scan-time ratio, spatial resolution, and image quality. In summary, the mix-TSE pulse sequence could become a powerful tool for clinical applications of quantitative MR imaging.

**CORRESPONDENCE TO**

Hernán Jara, PhD  
Radiologic Physics and Digital Imaging Systems  
ACC-4, 850 Harrison Avenue  
Boston University School of Medicine  
Boston Medical Center  
Boston, MA 02118  
E-mail: hjara@bu.edu  
Phone: (617) 414-7478  
Fax: (617) 414-7924

**References**

1. Bakker CJ, de Graaf CN, van Dijk P. Derivation of quantitative information in NMR imaging: a phantom study. *Physics in Medicine & Biology* 1984 Dec; 29(12):1511-25.
2. Schneiders NJ, Ford JJ, Bryan RN. Accurate T1 and spin density NMR images. *Medical Physics* 1985; 12(1):71-6.
3. Schneiders NJ, Post H, Brunner P, Ford J, Bryan RN, Willcott MR. Accurate T2 NMR images. *Medical Physics* 1983 Sept-Oct; 10(5):642-5.
4. Singer JR. NMR diffusion and flow measurements and an introduction to spin phase graphing. *Journal of Physics E* 1978; 11:281-291.
5. Le Bihan D, Breton E. Imagerie de diffusion in-vivo par resonance magnetique nucleaire. *Comptes Rendus de l'Academie des Sciences. Serie III, Sciences de la Vie* 1985; 301:1109-12.

6. Hennig J, Nauerth A, Friedburg H. RARE imaging: a fast imaging method for clinical MR. *Magnetic Resonance in Medicine* 1986 Dec; 3(6):823-33.
7. In den Kleaf JJ, Cuppen JJ. RLSQ: T1, T2, and rho calculations, combining ratios and least squares. *Magnetic Resonance in Medicine* 1987 Dec; 5(6):513-24.
8. Andersen C, Jensen FT. Precision, accuracy, and image plane uniformity in NMR relaxation time imaging on a 1.5 T whole-body MR imaging system. *Magnetic Resonance Imaging* 1994; 12(5):775-84.
9. Jara H. Synthetic Images for a Magnetic Resonance Imaging Scanner Using Linear Combination of Source Images to Generate Contrast and Spatial Navigation, United States Patent Application (Filing date: 02/08/2001).

**Author Information**

**Megan E Jensen, MS**

Department of Biomedical Engineering, College of Engineering, Boston University

**Shelton D Caruthers, PhD**

Director of Cardiovascular MR Labs, Washington University in St. Louis School of Medicine, Philips Medical Systems North America

**Hernán Jara, PhD**

Assistant Professor of Radiology / Adjunct Associate Professor of Biomedical Engineering, Radiologic Physics and Digital Imaging Systems / College of Engineering, Boston University Medical School and Boston Medical Center / Boston University